J Biosci (2020)45:77
DOI: 10.1007/s12038-020-00052-3

Atorvastatin ameliorates viral burden and neural stem/progenitor cell (NSPC) death in an experimental model of Japanese encephalitis

Masood Ahmad Wani[1,2], Sriparna Mukherjee[1,3], Suvadip Mallick[1,4], Irshad Akbar[1,5] and Anirban Basu[1]*

[1]*National Brain Research Centre, Manesar, Gurugram 122 052, India*

[2]*Present Address: Institute for Stem Cell Science and Regenerative Medicine, Bengaluru 560 065, India*

[3]*Present Address: Department of Pharmacology and Physiology, Pavilion Roger-Gaudry, Universite de Montréal, Montréal, Québec H3T 1J4, Canada*

[4]*Present Address: Tulane National Primate Research Center, 18703, Three Rivers Road, Covington, Louisiana 70433, USA*

[5]*Present Address: Department of Molecular Medicine, Faculty of Medicine, Université Laval, Québec G1V 4G2, Canada*

**Corresponding author (Email, anirban@nbrc.ac.in, anirban.nbrc@gmail.com)*

MS received 12 January 2020; accepted 16 May 2020

Japanese encephalitis virus, a neurotropic flavivirus, causes sporadic encephalitis with nearly 25% fatal case reports. JEV infects neural stem/progenitor cells (NSPCs) and decreases their proliferation. Statin, a commonly used class of cholesterol lowering drug, has been shown to possess potent anti-inflammatory and neuroprotective effects in acute brain injury and chronic neurodegenerative conditions. Here, we aimed to check the efficacy of atorvastatin in alleviating the symptoms of Japanese encephalitis (JE). Using BALB/c mouse model of JEV infection, we observed that atorvastatin effectively reduces viral load in the subventricular zone (SVZ) of infected pups and decreases the resultant cell death. Furthermore, atorvastatin abrogates microglial activation and production of proinflammatory cyto/chemokine production post JEV infection *in vivo*. It also reduced interferon-β response in the neurogenic environs. The neuroprotective role of atorvastatin is again evident from the rescued neurosphere size and decreased cell death *in vitro*. It has also been observed that upon atorvastatin administration, cell cycle regulatory proteins and cell survival proteins are also restored to their respective expression level as observed in uninfected animals. Thus the antiviral, immunomodulatory and neuroprotective roles of atorvastatin reflect in our experimental observations. Therefore, this drug broadens a path for future therapeutic measures against JEV infection.

Keywords. Atorvastatin; drug repurposing; *Japanese encephalitis virus*; neural stem/progenitor cell; neurotropic viruses; statins

Abbreviations: ATR, atorvastatin; JEV, Japanese encephalitis virus; NSPC, neural stem/progenitor cell

1. Introduction

Japanese encephalitis virus (JEV), a member of the genus *Flavivirus* (Schweitzer *et al.* 2009), is the leading cause of acute encephalitis in the Asia-Pacific region. Approximately 67,900 clinical cases of JE occur every year worldwide, of which 20–30% are fatal and 30-50% survivors develop significant neurological sequelae (Basu and Dutta 2017). Neuronal death in

Electronic supplementary material: The online version of this article (https://doi.org/10.1007/s12038-020-00052-3) contains supplementary material, which is available to authorized users.

Published online: 04 June 2020

Japanese encephalitis (JE) occurs through a combination of direct virus induced damage and bystander killing by activated microglia (Ghoshal *et al.* 2007). The CNS responds to the damages incurred to neurons by recruiting new cells at the site of injury from the resident populations of neural stem/progenitor cells (NSPC) (Arvidsson *et al.* 2002; Abrous *et al.* 2005). These multipotential cells reside in specific niches of the brain, in particular, the subventricular zone (SVZ) and the dentate gyrus (DG) of hippocampus and are present throughout life (Ma *et al.* 2009). In addition to the neurogenic functions, NSPCs endow in regulation and maintenance of CNS homeostasis under both physiological and pathophysiological conditions (Martino *et al.* 2014). We previously reported that JEV-infected NSPCs have retarded proliferative potential (Das and Basu 2008) and they eventually undergo apoptosis (Mukherjee *et al.* 2017). Thus, depletion of NSPC pool is thought to be one of the contributing factors that culminates in the neurological sequelae observed in JE survivors.

Several researches have been conducted in the past decade to find out therapeutic drugs or vaccines exerting antiviral effects on JEV (Ishikawa and Konishi 2015; Wang *et al.* 2017) yet only a few effective clinical trials are reported till date (Kumar *et al.* 2009, 2016; Turtle and Solomon 2018). Statins, a class of cholesterol lowering agents with anti-inflammatory effects (Aktas *et al.* 2003; Wang *et al.* 2014) has been used for the treatment of hyperlipidaemia and associated cardiovascular diseases. Statins have proven beneficial in treatment of many human diseases such as ischemic stroke (Amarenco *et al.* 2006), central nervous system (CNS) autoimmune disease (Chataway *et al.* 2014), and Alzheimer's disease (Sparks *et al.* 2002). In particular, Atorvastatin (ATR) has been reported to promote neural progenitor cell (NPC) proliferation in young adult rats after stroke by upregulating presenilin-1 and notch signalling activity (Chen *et al.* 2008). Furthermore, ATR is found to rejuvenate neural stem cells (NSC) following oxygen-glucose deprivation (OGD) (Choi *et al.* 2019). It is also known to protect motor neurons from oxidative damage (Lee *et al.* 2016). Neuroprotective effects of ATR are demonstrated in intracerebral haemorrhage (ICH) rat models (Seyfried *et al.* 2004). A low dose of atorvastatin induces angiogenesis, neurogenesis, synaptogenesis, and enhances functional recovery after middle cerebral artery occlusion in rats (Chen *et al.* 2003). It is also reported to have an inhibitory effect on influenza virus replication as well as enhancing cell viability following H1N1 infection (Mehrbod *et al.* 2014).

Previous report from our group demonstrated a promising neuroprotective role of ATR in JEV and *Chandipura virus* (CHPV) infected BALB/c mice. ATR conferred protection to neurons and abrogated inflammatory cytokine response (Mallick *et al.* 2019). Based on our preliminary findings, we wanted to investigate the effect of ATR post JEV infection on NSPCs. Here, we report that ATR effectively ameliorates JEV induced NSPC death in the SVZ region. Furthermore, the protective effects of ATR are associated with reduction of viral titre, abrogated microgliosis and decreased production of proinflammatory cyto/chemokines in the subventricular zone.

2. Material and methods

2.1 *Ethics statement*

Animal experiments were performed after obtaining approval from the Institutional Ethics Committee (IAEC) of National Brain Research Centre (Approval no. NBRC/IAEC/2017/128). BALB/c mice pups were housed together with their mothers under a 12-hour dark/ 12-hour light cycle at a constant temperature and humidity with food and water *ad libitum*. Guidelines on laboratory animal care and practice as defined by the CPCSEA (Committee for the Purpose of Control and Supervision of Experiments on Animals, Ministry of Environment and Forestry, Government of India) were strictly followed for all animal experiments and maintenance.

2.2 *Virus propagation*

GP78 strain of *Japanese encephalitis virus* (JEV) was propagated in 2-day-old suckling BALB/c mice pups. Upon the manifestation of infection symptoms, the pups were euthanized to collect their brains. Brains were homogenized in serum-free DMEM and centrifuged at 10,000*g* for 30 min to remove tissue debris followed by filtration through 0.22 μm sterile filter (Millipore, USA). To calculate viral titre, plaque assay was performed using the porcine stable kidney cell line. The viral filtrate was stored in small aliquots at −80°C and used for all *in vivo* and *in vitro* experiments.

2.3 *Plaque assay*

JEV titre was determined by plaque formation on PS cell monolayer. PS cells were seeded in a six well plate to around 70% confluency in 10% DMEM and then incubated in serum-free DMEM for 2 h. The cells were then inoculated with 10-fold serial dilutions of mouse brain homogenate and incubated for 2 h at 37°C. The inoculum was removed and cells were gently washed with PBS. A 3 ml overlay with MEM containing 10% FBS, 1% agarose and 100 µl cocktail of penicillin-streptomycin (Gibco, Invitrogen Corporation, USA) was poured onto each well. The plates were incubated at 37°C for 72–96 h. The cells were then fixed with 10% PFA for 4 h at room temperature and stained with crystal violet to visualize plaques.

2.4 *Atorvastatin formulation*

ATR (a kind gift from Sun Pharmaceuticals, India) was prepared as 80 mM stock in DMSO. This stock was diluted with 1X PBS to make a working dose of 5 mg/kg (approximately 50 µl per animal) and used for all *in vivo* experiments. For *in vitro* experiments a 10 mM stock of ATR was prepared in DMSO and all required concentrations were made from this stock.

2.5 *Virus infection and atorvastatin treatment in mice*

10-day-old (P10) BALB/c mice pups without sexual biasness were randomly assigned into 4 groups: Mock, only atorvastatin treated (ATR), JEV-infected (JEV), JEV-infected and atorvastatin treated (JEV+ATR). Pups of JEV group were intraperitoneally injected with 3×10^5 plaque-forming units (PFU) of JEV. Mock group received an equal volume of phosphate-buffered saline (PBS). In JEV+ATR group, Atorvastatin at a dose of 5 mg/kg body weight was administered intraperitoneally two hours post JEV infection and then after every 24 h for five consecutive days. Only Atorvastatin group received an equal dose of drug every time along with that of JEV+ATR group. From 5th day onwards JEV-infected animals started to show symptoms of JE including restriction of movements, poor pain response, whole body tremor, piloerection and hind limb paralysis. All the animals were sacrificed on 6th day post infection either for protein, RNA or immunohistochemistry (IHC). Brains collected for IHC were kept in 4% paraformaldehyde (PFA) at 4°C until sectioning.

For SVZ isolation, briefly, animals were euthanized and transcardially perfused with 1X ice cold PBS. Brains were removed and approximately 1mm thick coronal section were sliced $\sim$ 2 mm from the anterior pole of the brain. The sections were then placed in a petri dish containing PBS, in which SVZ was dissected out under microscope.

2.6 *Neurosphere culture from SVZ region*

SVZ from BALB/c mouse pup brains (post-natal day 7) was dissected out aseptically in ice chilled PGM buffer (Phosphate buffer with 1 mM MgCl2 and 0.6 % glucose) under microscope and minced mechanically. The tissue was then dissociated in 2 mg/ml papain solution with 50 µg/ml DNase I at 37°C for 10 min and neutralized with DMEM containing 10 % FBS. After centrifugation, the pellet was washed once with DMEM/F12 media (Gibco, USA) and re-suspended in DMEM/F12. The suspension was kept for 2 min to allow the large debris to settle down. This step was repeated twice. The supernatants were pooled and centrifuged at 1000 rpm for 5 min. The pellet was then suspended in DMEM/F12 media supplemented with B27, N2, 20 mg/ml EGF (Epidermal Growth Factor; R&D Systems, Minneapolis) and 10 mg/ml FGF (Fibroblast Growth Factor; R&D Systems, Minneapolis) and plated at a density of 3×10^5 cells/ml. Fresh media was added after every 2 days. All the experiments were carried out after minimum 2 passages and under cell density of 0.2×10^6 cells/ml in 6-well plates.

2.7 *JEV infection and ATR treatment in neurospheres*

Mouse neurospheres after two passages were seeded for following six conditions: Mock, 1.5 µM ATR, 2.0 µM ATR, JEV, JEV+ATR 1.5 µM, JEV+ATR 2 µM. JEV infection was given at 1 MOI on 3rd day when spheres start to from and two hours post infection atorvastatin was added at respective doses. The spheres were imaged 72 h post-infection for diameter analysis. In other set of experiments, spheres were adhered on Poly-D-lysine (PDL, Sigma) coated 8 well chamber slides and fixed with 4 % PFA for Immunocytochemistry (ICC).

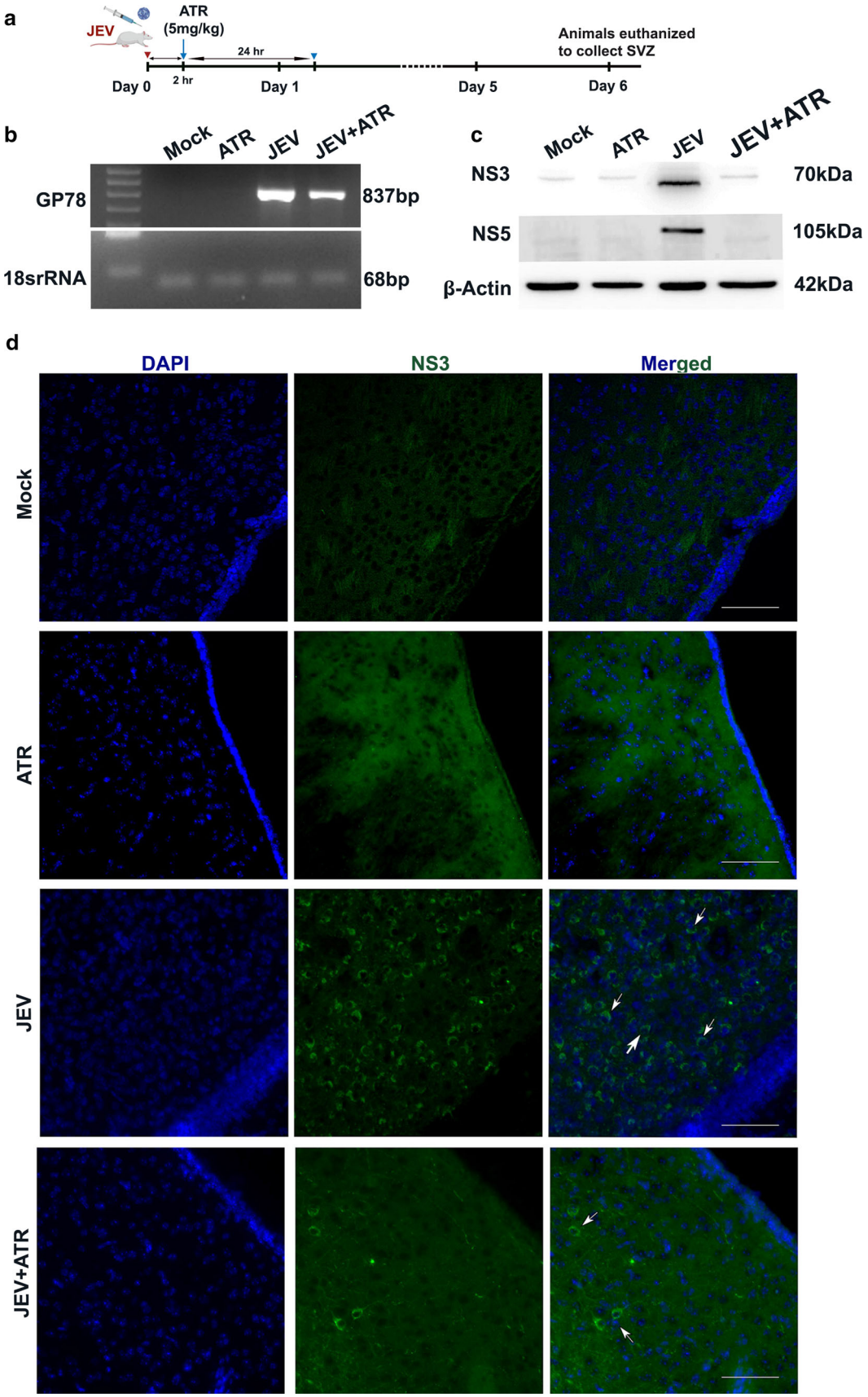
a
JEV
ATR
(5mg/kg)
24 hr
2 hr
Day 0
Day 1
Day 5
Day 6
Animals euthanized
to collect SVZ
b
Mock
ATR
JEV
JEV+ATR
GP78
837bp
18srRNA
68bp
c
Mock
ATR
JEV
JEV+ATR
NS3
70kDa
NS5
105kDa
β-Actin
42kDa
d
DAPI
NS3
Merged
Mock
ATR
JEV
JEV+ATR

◀**Figure 1.** Atorvastatin reduces viral load *in vivo*. (**a**) Experimental scheme showing JEV and ATR treatment paradigm in 10-day old BALB/c mice pups. Pups of JEV group were intraperitoneally injected with 3×10^5 plaque-forming units (PFU) of the virus. In JEV+ATR group, ATR at a dose of 5 mg/kg body weight was administered IP 2 hours post infection and then after every 24 hours for 5 consecutive days. All animals were sacrificed on day 6. 4 animals per experimental group were used. (**b**) The expression of JEV mRNA in the SVZ of Mock, ATR, JEV and JEV+ATR mice pups were assessed by semi-quantitative RT-PCR followed by visualization in agarose gel. (**c**) Immunoblot analysis of JEV non-structural protein 3 (NS3) and non-structural protein 5 (NS5) in the SVZ of all four experimental groups. (**d**) Immunostaining images of JEV NS3 in the SVZ region (NS3: green, DAPI: Blue). Magnification 20X; scale bar corresponds to 50μm. Data are representative of three independent experiments.

2.8 *Neurosphere culture from JEV-infected and atorvastatin treated animals*

SVZ isolated from all four groups (described earlier) were processed for neurosphere culture. Single cell suspension was prepared from SVZ region of the experimental groups and cells were seeded at density of 0.2×10^6 cells/ml in 6-well cluster plates for the respective four groups. The spheres were imaged on 7th day of culture for diameter analysis. In other set of experiments, spheres were adhered on Poly-D-lysine (PDL)-coated 8-well chamber slides and fixed with 4 % PFA for Immunocytochemistry (ICC).

2.9 *Immunocytochemistry*

PFA fixed neurospheres were washed with 1X PBS and permeabilized with 0.1% PBXT (Triton X-100) for 20 min at RT. This was followed by blocking for 3 hours at RT in blocking solution containing 10% serum (prepared in 0.01% PBXT) of animal in which secondary antibody was raised. Primary antibodies were prepared in 5% serum in 0.01% PBXT and incubated overnight in a humidified chamber at 4°C. Antibodies against nestin (Merck Millipore, 1:100) and caspase-3 (Cell signaling, 1:200) were used. After 5-6 PBXT washes, the corresponding fluorochrome conjugated secondary antibodies were added for 1.5 hour (Alexa Fluor 488, Alexa Fluor 594, 1:1000, Invitrogen Molecular Probes, USA) at room temperature (RT). After 5–6 PBXT washes, slides were mounted with Vectashield mounting medium for fluorescence with DAPI (Vector Labs). Images were captured using Zeiss Apotome microscope (Zeiss, Germany).

2.10 *Immunohistochemistry*

PFA fixed brains from all four animal groups were kept in 30% sucrose for 3–4 days. Serial SVZ sections (20 μm) were obtained in Leica CM3050 S Cryostat and were stored in -30°C until use. Antigen retrieval was done using Antigen Unmasking Solution (Vector Labs) in boiling water bath for 30 min. The sections were brought to room temperature, washed with PBS. Following washes with PBS, the sections were permeabilized with 0.2% PBXT (Triton X) for 30 min and then incubated for 3 h in blocking solution containing 10% serum (prepared in 0.01% PBXT) of the animal in which secondary antibody was raised. Primary antibodies against nestin (Merck Millipore, 1:100) and caspase-3 (Cell signaling, 1:200) were then added and left overnight in a humidified chamber at 4°C. Following 5–6 washes with PBXT, the sections were incubated with suitable fluorochrome conjugated secondary antibodies (Alexa Fluor 488, Alexa Fluor 594, 1:1000 Invitrogen Molecular Probes, USA) at RT for 1.5 h. After 5–6 washes, slides are mounted with Vectashield mounting medium for fluorescence with DAPI (Vector Labs). Images were captured using Zeiss Apotome microscope (Zeiss, Germany).

2.11 *Immunoblotting*

The SVZ tissue was homogenized in complete lysis buffer (1% Triton X-100, 10 mM tris-HCl (pH 8.0), 150 mM NaCl, 0.5% NP-40, 1 mM EDTA, 0.2% EGTA, 0.2% sodium orthovanadate, and a protease inhibitor cocktail (Sigma-Aldrich)) and centrifuged at 12,000 rpm for 30 min. The supernatant was collected and quantified by bicinchoninic acid method. 30 μg of each of the sample was separated in SDS PAGE followed by transfer onto a nitrocellulose membrane. The blots were blocked with 10% non-fat milk for 3 h and incubated with primary antibodies overnight at 4°C against JEV non-structural protein 3 (Genetex, 1: 10,000), Caspase-3 (Cell signaling, 1:2000), mouse Cleaved Caspase-8 (Cell signaling, 1:1000), Caspase-9 (Cell signaling, 1:2000), Cleaved PARP1 (Abcam, 1:5000), Prohibitin (Abcam, 1:1000), Phospho-Akt (Cell signaling, 1:1000), Akt (Cell signaling, 1:1000),

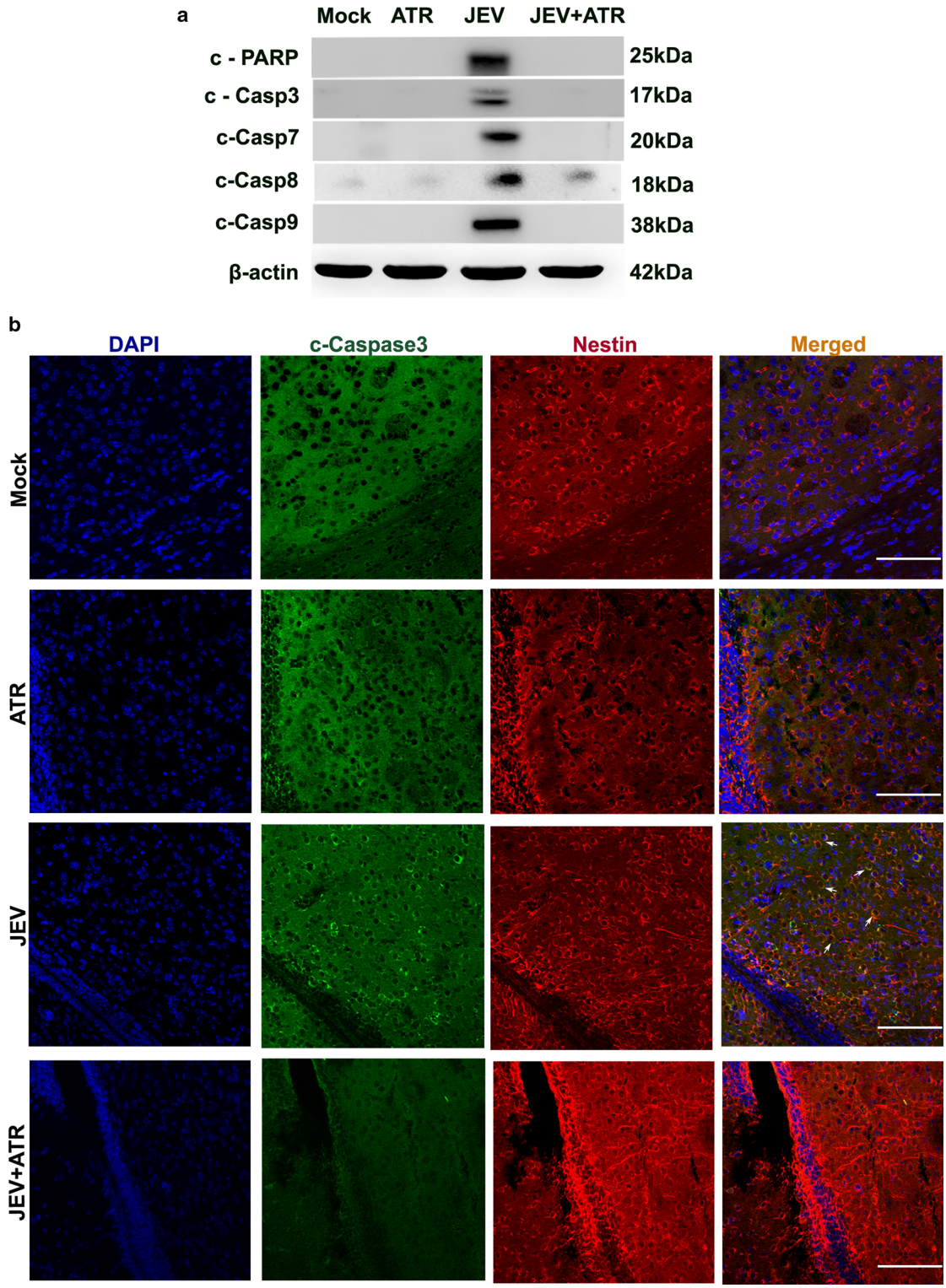

Figure 2. Atorvastatin ameliorates neural stem/progenitor cell (NSPC) death in the mouse subventricular zone. (**a**) Immunoblot analysis of caspases and Cleaved-Poly-ADP-ribose polymerase (cPARP) expression in the SVZ of Mock, ATR, JEV and JEV+ATR groups. (**b**) Representative images of double-immunofluorescence staining for Nestin and cleaved-Caspase 3 in the SVZ region. Magnification 20X; scale bar corresponds to 50μm. Data are representative of three independent experiments.

Phospho-p53 (Cell signaling, 1:1000), p27 (Abcam, 1:500). β-actin was used as internal control for loading (Sigma-Aldrich, 1: 10,000). After 5-6 TBST (1X Tris buffered saline with Tween 20) washes, blots were incubated with respective HRP-conjugated secondary antibodies (1:7500, Vector Laboratories, USA) followed by washing and developing through ECL kit (Millipore, CA, USA). Images were captured in UVITECH imaging system, Cambridge.

2.12 *RNA isolation and semi quantitative PCR*

Total RNA was extracted from SVZ tissue by Trizol (Sigma) reagent followed by chloroform and isopropanol treatment. The RNA pellet was washed with 70% ethanol, air dried and resuspended in RNase free water. cDNA was synthesized from 500 ng of RNA using Verso cDNA Synthesis Kit (Thermo Fisher Scientific, Waltham, MA USA) as per the manufacturer's protocol. The cDNA prepared was subjected to semi-quantitative PCR. Primer sequence used to amplify JEV GP78 are F 5′-TTGACAATCATGGCAAACG-3′ R 5′-CCCAACTTGCGCTGAATAA-3′ and for mouse 18s rRNA (used as an internal control) are F 5′-GA GGGAGCCTGAGAAACGG-3′ R 5′-GTCGGGAGT GGGTAATTTGC-3′. The amplified products were run on 2% agarose gel containing 0.01% Ethidium Bromide (EtBr) and imaged in UVITECH imaging system, Cambridge.

2.13 *Quantitative RT-PCR*

For quantitative determination of mature mRNA abundances in *in vivo* samples, qRT-PCR analysis was performed. cDNA was prepared as per protocol mentioned earlier and diluted with MilliQ in 1:5 ratios. qRT-PCR analysis of mouse IFN-α, IFN-β and IFN-γ were performed with the Power SYBR Green PCR Master Mix (Applied Biosystems) with gene-specific primer: IFN-α F 5′-ATTGGCTAGGCTCTGTGCTT T-3′ R5′AGGGCTCTCCAGACTTCTGC -3′; IFN-β F5′-AAGAGTTACACTGCCTTTGCCATC-3′ R5′-AG GGCTCTCCAGACTTCTGC-3′; IFN-γ F5′-TCAAG TGGCATAGATGTGGAAGAA-3′ R5′TGGCTCTGC AGGATTTTCATG-3′. The relative abundance of mRNA of interest was determined by normalization to that of GAPDH mRNA through the $2^{-\Delta\Delta Ct}$ method. Primer sequence of mouse GAPDH used are F 5′-A TGGCAAGTTCAAAGGCACAGTC-3′ R 5′-TGGG GGCATCAGCAGAAGG-3′.

2.14 *Cytokine bead array*

Abundance of inflammatory cytokines were measured in mouse subventricular zone in all four groups by flow cytometry using BD™ Cytometric bead array mouse inflammation kit (BD Biosciences) as per the manufacturer's instructions. Data were obtained and analyzed in FACS Verse™ (Becton Dickinson, San Diego, CA, USA).

2.15 *Statistical analysis*

All experiments are performed in triplicate unless otherwise stated and data are expressed as mean ± SD. Results were analyzed for statistical significance by one-way ANOVA followed by Tukey *post hoc* test. All statistical analyses were performed using GraphPad Prism (GraphPad Software, San Diego) and differences with $p<0.05$ was considered statistically significant.

3. Results

3.1 *Atorvastatin reduces mRNA transcript of JEV and viral load in vivo*

Previous studies from our group demonstrated enhanced survivability and reduced viral titre in brains of mice pups infected with CHPV and JEV following atorvastatin treatment (Mallick *et al.* 2019). To investigate whether ATR can also reduce viral load in the subventricular zone (SVZ), we treated JEV-infected BALB/c mice pups with ATR at a dose of 5mg/kg body weight two hours post infection once daily through intraperitoneal route as done earlier (figure 1a). RNA was isolated from the SVZ region of the experimental groups and the expression of viral RNA was assessed by semi-quantitative PCR followed by visualization through agarose gel electrophoresis. The expression of JEV mRNA was reduced significantly in the SVZ of ATR treated mice pups compared to only JEV-infected pups (figure 1b). The observation was validated at the protein level by performing western blot for JEV non-structural protein 3 (NS3) and non-structural protein 5 (NS5) and similar results were obtained (figure 1c). To further validate, we immunostained NS3 in the SVZ to investigate the abundance of the virus. We found a profound reduction of JEV NS3 antigen in JEV+ATR mice SVZ compared to the only JEV-infected group (figure 1d). These findings demonstrate antiviral activity of atorvastatin in the subventricular zone.

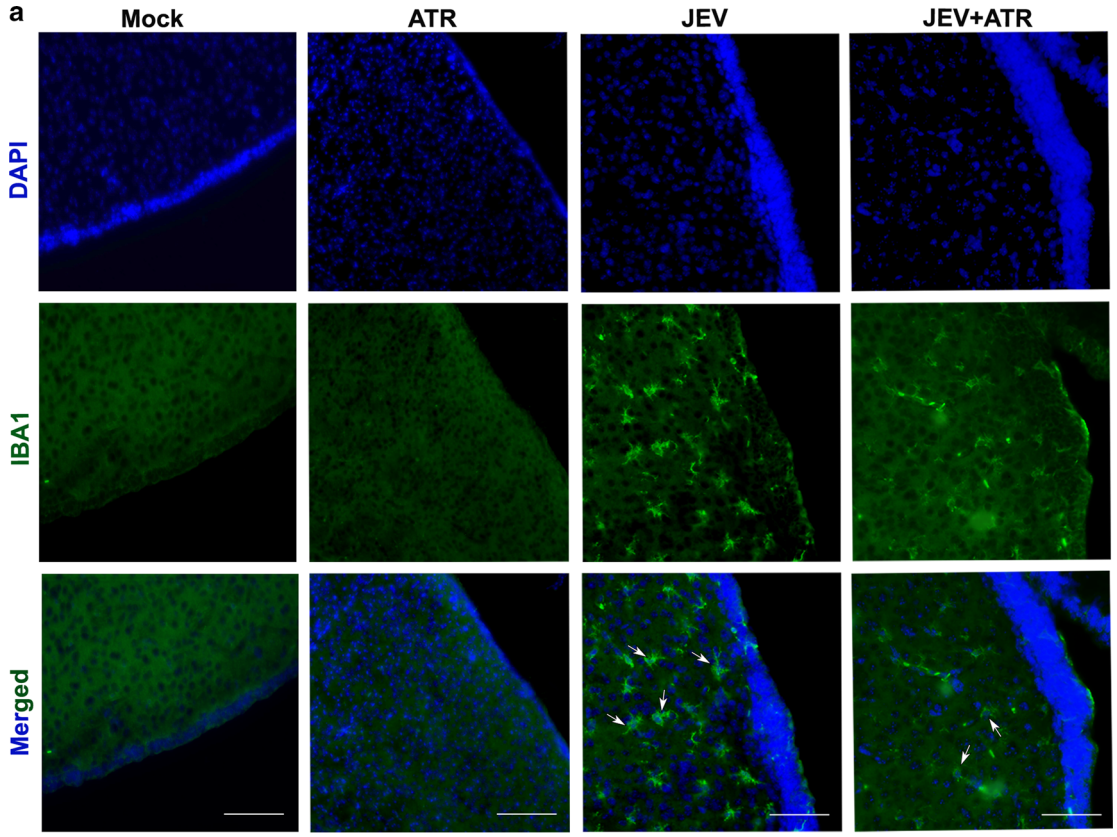
a
Mock
ATR
JEV
JEV+ATR
DAPI
IBA1
Merged

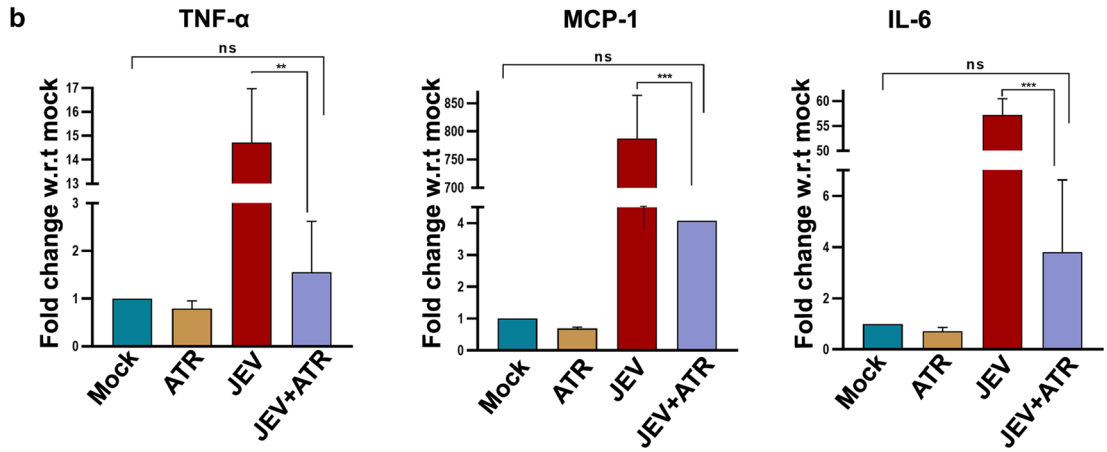
b
TNF-α
MCP-1
IL-6
Fold change w.r.t mock
ns
**
***
Mock
ATR
JEV
JEV+ATR

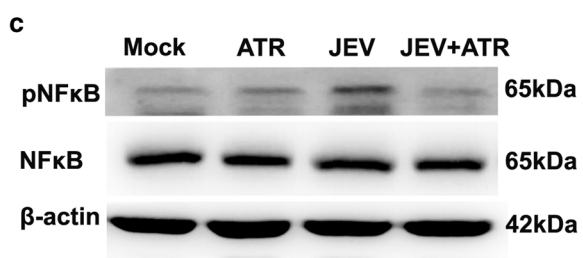
c
Mock
ATR
JEV
JEV+ATR
pNFκB
NFκB
β-actin
65kDa
65kDa
42kDa

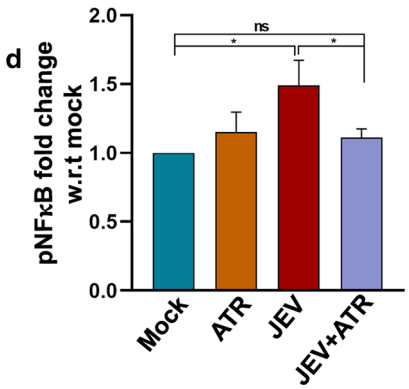
d
pNFκB fold change w.r.t mock
ns
*
*
Mock
ATR
JEV
JEV+ATR

◀**Figure 3.** Atorvastatin reduces microglial activation and proinflammatory cyto/chemokine production in the subventricular zone. (**a**) Immunostaining images of IBA-1 in the SVZ of Mock, ATR, JEV and JEV+ATR groups (IBA-1: Green, DAPI: Blue). Magnification 20X; scale bar corresponds to 50μm. (**b**) Cytokine bead array of proinflammatory mediators: Tumor Necrosis Factor-α (TNF-α), Macrophage chemoattractant protein (MCP-1) and Interleukin 6 (IL-6) levels in the SVZ from all four experimental groups. Data represents mean ± SD, representative of three independent experiments (**p<0.01 ***p<0.001; ns: non-significant). (**c**) Western blot analyses of pNFκB in the SVZ region and (d) Histogram showing pNFkB fold change in the experimental group compared to Mock (*p<0.05, ns: non-significant). 4 animals per experimental group were used in each experiment. Data are representative of three independent experiments, mean ± SD.

3.2 *Atorvastatin prevents JEV-induced NSPC apoptosis*

JEV was found to cause cell death in the SVZ region of mice pups and also in human neural stem\progenitor cells (Mukherjee *et al.* 2017). Therefore, in order to assess whether atorvastatin can protect NSPCs from JEV induced apoptosis, we investigated the expression levels of cleaved caspases in the subventricular zone. Immunoblot analysis showed elevated expression of cleaved caspases and cPARP, indicative of cellular apoptosis, in JEV-infected mice SVZ, all of which were significantly reduced in JEV+ATR group (figure 2a). To validate further, we immunostained the SVZ regions with Nestin and cleaved-Caspase 3. We found their extensive colocalization in the SVZ of JEV-infected group which was found to be markedly reduced in JEV+ATR group (figure 2b).

3.3 *Atorvastatin abrogates microglial activation and inflammation in vivo*

Increased microglial activation and the ensuing upheaval of proinflammatory mediators are considered to be the hallmarks of JEV infection (Ghoshal *et al.* 2007). We, therefore, looked for microglial activation and proinflammatory cyto/chemokine production in the SVZ following ATR treatment. Immunostaining of SVZ sections from JEV-infected group showed elevated IBA1 expression indicative of activated microglia when compared to Mock, which was noticeably reduced in JEV+ATR group (figure 3a). In another set of experiments, SVZ was dissected out from all four experimental groups and Cytokine Bead Array (CBA) was performed to analyze changes in proinflammatory cyto/chemokine levels in the SVZ after ATR treatment. Tumor Necrosis Factor-α (TNF-α) showed a significant 14-fold increase in JEV-infected group compared to Mock ($p<0.01$), which was markedly reduced to 1.5-fold increase over Mock in JEV+ATR group. In case of chemokine, Macrophage chemoattractant protein (MCP-1) a dramatic 780-fold increase over Mock is observed in JEV group ($p<0.001$) but reduced significantly in JEV+ATR group (a 4-fold increase over Mock). Interleukin 6 (IL-6) levels after atorvastatin treatment in JEV+ATR group was greatly decreased to 3.8-fold when compared to 57-fold increase in JEV group over Mock ($p<0.001$) (figure 3b). The expression of these proinflammatory molecules is known to be modulated by NFκB which serves as a central mediator of inflammatory responses. There was a distinct 1.5-fold increase in pNFκB levels in the SVZ of JEV-infected animals compared to Mock, which was markedly reduced in JEV+ATR group ($p<0.05$) (figure 3c and d).

3.4 *Impaired neurosphere formation upon JEV infection is rescued by Atorvastatin*

JEV has been reported to affect neurosphere formation *in vitro*, attributed to its potential to limit the proliferative capacity of NSPCs (Das and Basu 2008). To test whether ATR can rescue the impaired neurosphere formation upon JEV infection, we treated neurospheres cultured from SVZ of 7-day-old mice pups with atorvastatin (1.5 μM, 2.0 μM) after a minimum of two passages. NSPCs were infected with JEV on 3rd day and ATR was added two hours post infection at respective mentioned doses. After 72 hours of infection, bright field images were captured (Nikon Eclipse T*i*-S) and diameter analysis was performed using ImageJ (NIH, USA). The average sphere diameter of NSPCs infected with JEV was in the range of 20–25 μm which was significantly smaller than Mock neurospheres with sphere size in the range of 45–50 μm. NSPCs infected with JEV and treated with ATR, however, resulted in spheres with an average diameter of range 35–45 μm which was greater than those of infected with JEV ($p<0.01$) and at par to those of Mock neurospheres (figure 4a and b). NSPCs treated with only ATR (1.5 μM, 2.0 μM) showed minute change in sphere size compared to Mock suggesting ATR has negligible effect on NSPC proliferation *in vitro*. To check whether ATR also abrogates JEV

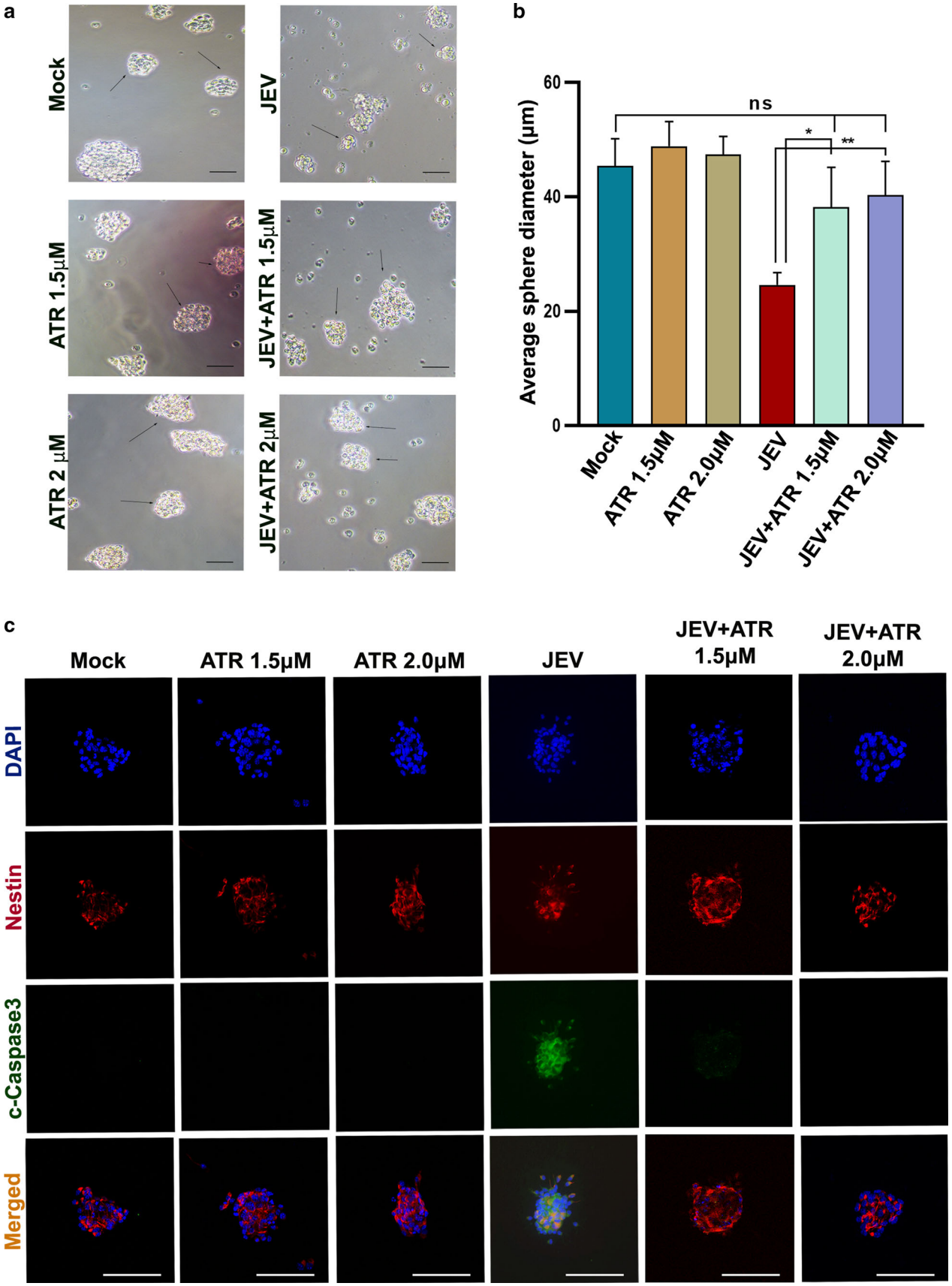
a
Mock
JEV
ATR 1.5μM
JEV+ATR 1.5μM
ATR 2 μM
JEV+ATR 2μM
b
Average sphere diameter (μm)
60
40
20
0
ns
*
**
Mock
ATR 1.5μM
ATR 2.0μM
JEV
JEV+ATR 1.5μM
JEV+ATR 2.0μM
c
Mock
ATR 1.5μM
ATR 2.0μM
JEV
JEV+ATR 1.5μM
JEV+ATR 2.0μM
DAPI
Nestin
c-Caspase3
Merged

◀**Figure 4.** Impaired neurosphere formation upon JEV infection is improved by atorvastatin treatment. (**a**) Phase contrast images of neurospheres grown for the following conditions: Mock, ATR 1.5 μM, ATR 2.0 μM, JEV, JEV+ATR 1.5 μM, JEV+ATR 2.0 μM. Magnification 10X; scale bar corresponds to 100μm. (**b**) Average sphere diameter (μm) histogram plotted for mentioned six conditions. Values represent mean ± SD from 3 independent experiments (*p<0.05, **p<0.01; ns: non-significant). (**c**) Double-immunofluorescence staining images of neurospheres for Nestin and cleaved-Caspase 3. Magnification 20X; scale bar corresponds to 50μm. Data are representative of three independent experiments.

induced NSPC apoptosis, we immunostained neurospheres with Nestin and cleaved-Caspase 3. JEV-infected neurospheres showed extensive colocalization of both, indicative of NSPC apoptosis. However, the JEV+ATR neurospheres showed lesser colocalization of them when compared to JEV-infected spheres (figure 4c).

3.5 *Stunted neurospheres from JEV-infected animals are rescued following Atorvastatin treatment*

We further validated our previous findings by culturing neurospheres directly from the SVZ of animals infected with JEV or treated with ATR. A minimum of 4 animals per experimental group were used for culture and the results are representative of three independent experiments. The spheres were imaged on the 7th day post plating and diameter was analyzed using ImageJ software (NIH, USA). The neurospheres cultured from JEV-infected pups had an average diameter in the range of 50–65 μm which was significantly smaller in size when compared to spheres cultured from the Mock group (120-145μm). The average sphere diameter, however, of neurospheres cultured from JEV+ATR pups were significantly greater (105–130 μm) when compared to JEV-infected group (p<0.001) but at par to those of Mock neurospheres (figure 5a and b). The neurospheres cultured from only ATR treated animals had sphere size at par to those of Mock suggesting no effect of ATR on NSPCs *in vivo*. We immunostained these neurospheres for Nestin and cleaved-Caspase 3. Neurospheres from JEV-infected mice pups showed their colocalization, indicative of NSPC apoptosis. However, the neurospheres from JEV+ATR group showed lesser co-localization when compared to the JEV-infected group (figure 5c).

3.6 *Atorvastatin regulates Akt signaling pathway associated with survival and proliferation and facilitates cell cycle progression in vivo*

Akt pathway is important in the survival and proliferation of stem cells (Song *et al.* 2005). Atorvastatin has been reported to restore normal Akt signalling protein levels in NSC under oxygen and glucose deprivation (OGD) which is known to cause cerebral infarction and ischemic stroke (Choi *et al.* 2019). We, therefore, checked phosphorylation levels of Akt in the SVZ region. Western blot analysis showed significant 3-fold downregulation of pAkt in the SVZ of JEV-infected mouse pups compared to Mock (p< 0.05). However, it was comparable to Mock in JEV+ATR group (figure 6a and b). JEV is known to modulate various checkpoint proteins involved in cell cycle progression that eventually results in suppression of NSPC proliferation (Das and Basu 2008). We, therefore, investigated the status of key cell cycle regulatory proteins following atorvastatin treatment. P-p53 and p27 proteins were found to be upregulated in SVZ of JEV-infected animals, 1.75- and 1.65-fold increase over Mock respectively (p<0.05). However, these were reduced significantly in JEV+ATR group when compared to only JEV-infected group (p<0.05) (figure 6e and f).

Prohibitin (PHB) is a mitochondrial membrane protein and has previously been reported from our group for its role in the recognition of JEV RNA (Mukherjee *et al.* 2017). PHB has also been found to bind p53 and induce its transcriptional activity (Fusaro *et al.* 2003). PHB expression was studied after ATR treatment in JEV-infected animals. As anticipated, immunoblot analysis revealed elevated PHB expression in the JEV-infected SVZ (a 2.7-fold increase over Mock) which is significantly reduced after ATR treatment (p<0.05) (figure 6c and d).

3.7 *Heightened IFN- β response following JEV infection is attenuated by Atorvastatin treatment in vivo*

Interferons are host defence response to combat viral infections. JEV is known to elicit neuronal innate immune response following viral recognition through RIG-1 and TLR7 signalling which has been shown to produce type-I interferons (Nazmi *et al.* 2011, 2014). We found that JEV infection led to a substantial 6-fold increase in IFN-β mRNA abundance in the SVZ compared to Mock (p<0.001), as analysed by qRT-PCR, which was markedly reduced following

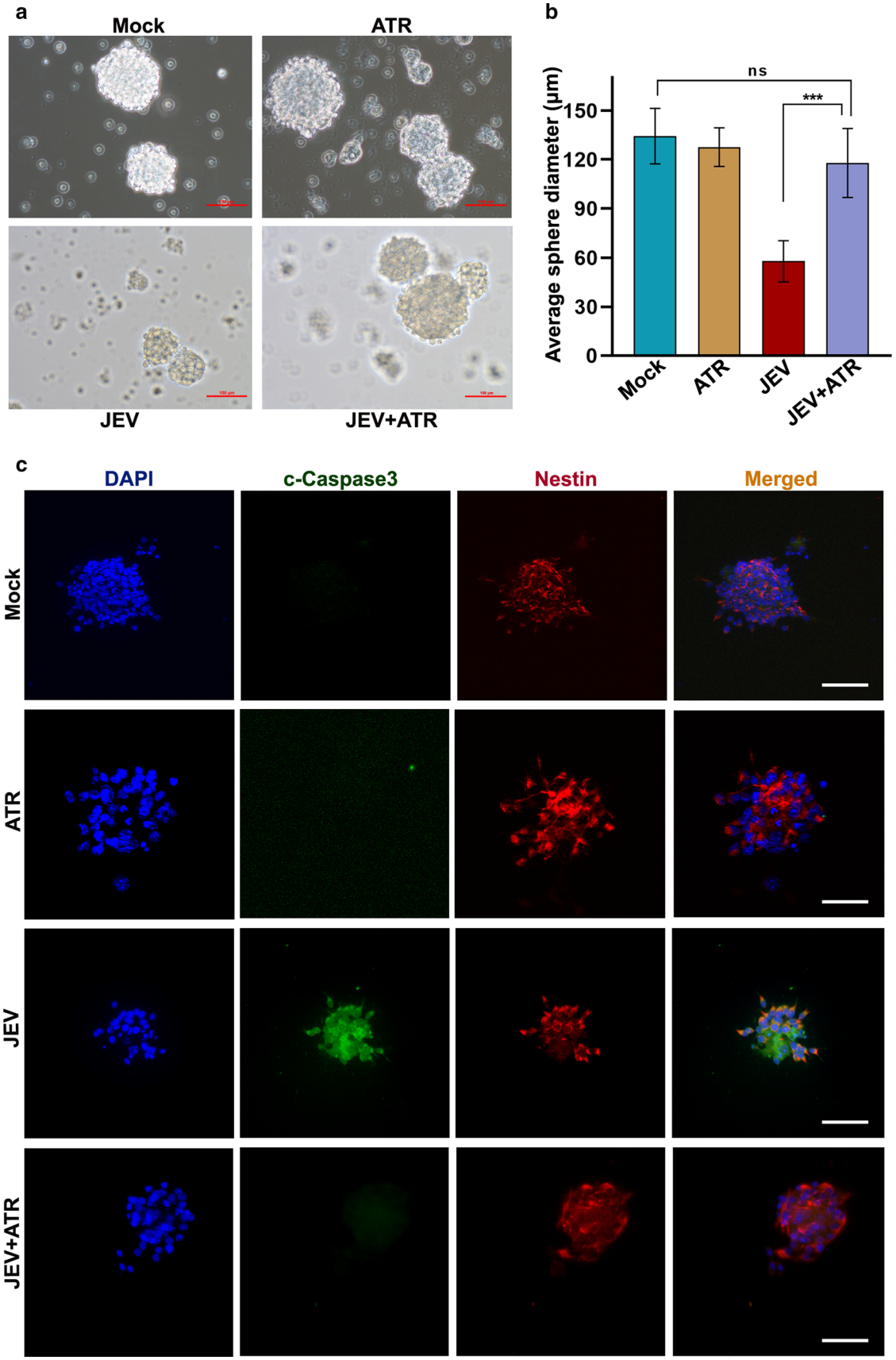
a
Mock
ATR
JEV
JEV+ATR
b
Average sphere diameter (µm)
ns
***
150
120
90
60
30
0
Mock
ATR
JEV
JEV+ATR
c
DAPI
c-Caspase3
Nestin
Merged
Mock
ATR
JEV
JEV+ATR

◀**Figure 5.** Impaired neurosphere formation from JEV-infected animals is rescued in atorvastatin treated group. (**a**) Bright field images of neurospheres cultured from Mock, ATR, JEV and JEV+ATR mice pups. Magnification 10X; scale bar corresponds to 100μm. Images shown in this Figure are representative of four individual animals from each group (**b**) Average sphere diameter (μm) histogram plotted for the mentioned experimental groups. Values represent mean ± SD (***$p<0.001$; ns: non-significant). (**c**) Double-immunofluorescence staining images of neurospheres cultured from SVZ region of mentioned groups for Nestin and cleaved-Caspase 3. Magnification 20X; scale bar corresponds to 50μm. 4 animals per experimental group were used. Data are representative of three independent experiments.

atorvastatin treatment (figure 7a). The amount of secreted IFN-β was also increased to 4-fold over Mock as determined by enzyme-linked immunosorbent assay (ELISA) in proteins isolated from SVZ of JEV-infected animals ($p<0.01$). Upon ATR treatment, the level was significantly reduced when compared to the JEV-infected group ($p<0.05$) (figure 7b). However, we found no difference in the mRNA expression level of IFN-α and IFN-γ in the subventricular zone of all experimental groups (supplementary figure 1a and b).

4. Discussion

The two canonical neurogenic areas in the mammalian brain, the SVZ around the lateral ventricles and SGZ in the hippocampus, serves as a reservoir of actively proliferating multipotential cells (Göritz and Frisén 2012). A dynamic NSPC pool is critical during brain recovery as the brain responds to any neuronal damage by differentiating and recruiting new neurons to the site of insult from the neurogenic niche (Niimi and Levison 2018) (Martí-Fàbregas *et al.* 2010). JEV is well known to infect NSPCs which in the long run might gradually cause waning of the brain's potential to repair damages due to various insults. One of the pathological hallmarks of JEV infection is the severe brain inflammation, to which NSCs are highly vulnerable (Ekdahl *et al.* 2003) (Iosif *et al.* 2006). Therefore, an effective therapeutic intervention would highlight the prerequisite of protecting NSPCs following the viral challenge. Preliminary studies from our group reported enhanced survivability up to 80% in animals infected with JEV following atorvastatin treatment and its effectiveness in curtailing the cyto/chemokine storm that follows leading to improvements in clinical severity of the disease (Mallick *et al.* 2019). ATR also rescued body weight loss as observed in only JEV-infected animals in the same study. The only ATR group animals showed minimal differences in body weight compared to Mock suggesting that the drug doses used in all *in vivo* experiments does not have any significant effect on animal's physiology. Since atorvastatin has diverse protective effects on neural stem cells, we studied its efficacy in the amelioration of NSPC death following JEV infection. The principal findings of this study are: (1) Atorvastatin reduces viral load and ameliorates NSPC death in the mouse SVZ. (2) ATR abrogates microglial activation and production of proinflammatory cyto/chemokine production post-JEV infection *in vivo*.

JEV targets brain-resident macrophage – microglia, activates it and leads to an exaggerated immune response in the form of a cytokine surge which is considered to be the key contributor to morbidity and mortality in JE (Ghoshal *et al.* 2007). Thus, effective drug therapy for JEV infection would aim to blunt such innate inflammatory responses to improve disease pathology. pNFκB is the central modulator of various proinflammatory genes (Shih *et al.* 2015). We found that upon JEV infection the pNFκB expression is increased in the SVZ. This increased expression of pNFκB might partly explain the elevated proinflammatory cyto/chemokines in the SVZ of JEV-infected animal. Following atorvastatin treatment, the level of pNFκB is markedly reduced compared to only JEV-infected group, which supports our observation that ATR reduces the production of proinflammatory molecules in the SVZ. Interleukin-6 (IL-6) is a proinflammatory cytokine which is found to be increased >50 folds in the JEV-infected SVZ. IL-6 is reported to play a critical role in the pathogenesis of several neuroinflammatory diseases and neurodegenerative diseases such as multiple sclerosis (MS), Parkinson's and Alzheimer's disease (Dufek *et al.* 2015). In the context of NSPCs, IL-6 presents both beneficial and detrimental effects. *In vivo studies* have shown that IL-6 treatment can have a prolonged effect on NSPC activity which may alter the cellular dynamics of the brain in the longer run. A brief surge in circulating IL-6 initially induces proliferation in NSPCs but cause long term depletion of neural stem cell pool (Storer *et al.* 2018). A decline in IL-6 levels after ATR treatment thus possibly deems advantageous for NSPC health. In most *in vivo* studies, TNF-α is reported to promote gliogenesis but limit neurogenesis (Borsini *et al.* 2015). Microglia-derived TNF-α is seen to exacerbate the death of hippocampal progenitor cells *in vitro* (Cacci

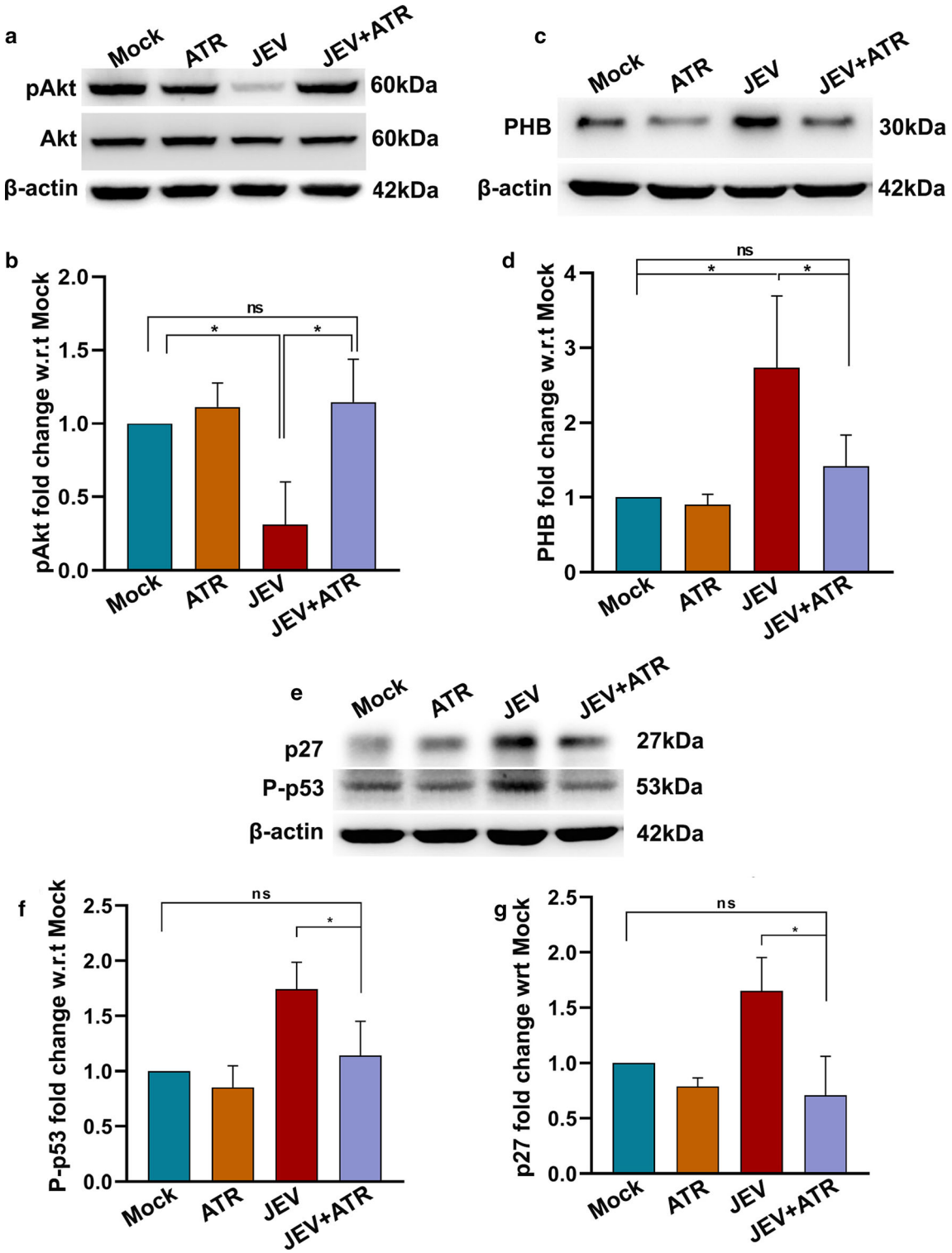

Figure 6. Atorvastatin modulates Akt signaling pathway and cell cycle checkpoint proteins in the SVZ region. (**a**) Western blot analysis of pAkt and total Akt in the SVZ of Mock, ATR, JEV and JEV+ATR groups. (**b**) histogram shows fold change in pAkt protein abundances (normalized to that of total Akt) in the experimental groups with respect to Mock. (**c**) Immunoblot analysis of Prohibitin (PHB) in the SVZ region of all four experimental groups. (**d**) Histogram showing densitometric analysis to determine fold change in PHB protein expression in the experimental groups compared to Mock. (**e**) Immunoblot analysis of P-p53 and p27 in the SVZ region. (**f,g**) Histogram shows fold change of P-p53 and p27 in the experimental groups compared to Mock. Values represent mean ± SD (*p<0.05; ns: non-significant). In each set of experiment, 4 animals per experimental group were used. Data are representative of three independent experiments.

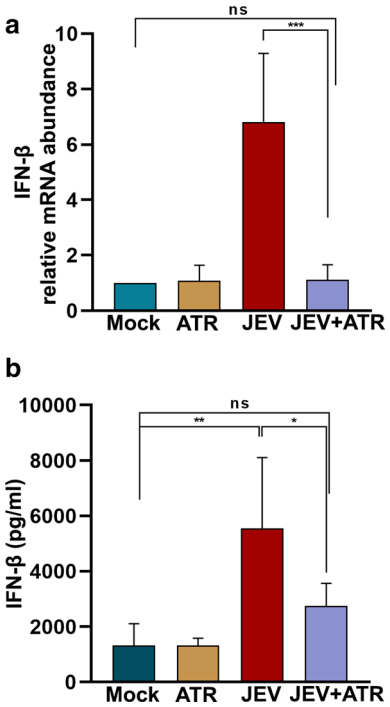

Figure 7. Atorvastatin reduces interferon-beta response *in vivo* following JEV infection. (**a**) qRT-PCR analysis of IFN-β mRNA in the SVZ of Mock, ATR, JEV and JEV+ATR groups. Values represent mean ± SD (***p<0.001; ns: non-significant). (**b**) Protein isolated from SVZ of all four groups were analyzed by ELISA in order to determine the amount of secreted IFN-β. Values represent mean ± SD (*p<0.05, **p<0.01; ns: non-significant). In each set of experiment, 4 animals per experimental group were used Data are representative of three independent experiments.

et al. 2005), whereas an *in vivo* loss of TNF-receptor function increases the number of new hippocampal neurons (Iosif 2006). JEV is known to causes impairment in neuronal differentiation of NSPCs likely through increased production of anti-neurogenic cytokines such as TNF-α (Das *et al.* 2011). ATR reduced TNF-α level multifold in SVZ of JEV-infected animal further corroborating its protective effects on NSPCs. MCP-1 levels were found to be significantly elevated following JEV infection and ATR treatment prominently reduced its expression in the SVZ.

We validated the findings *in vitro* using neurosphere cultures. We found that ATR treatment noticeably increased sphere size compared to only infected NSPCs suggesting that ATR possibly resumes the proliferative potential of NSPCs. To generate a more robust view of ATR-mediated protection, we analysed neurosphere sizes cultured directly from the SVZ of animals either infected with JEV or treated with ATR. We observed a similar pattern of increase in sphere sizes after ATR treatment, further validating our previous observation. Cell cycle arrest molecules are known to be upregulated in NSPCs following JEV infection (Das and Basu 2008) and since ATR prominently resumes proliferation of neurospheres we investigated the status of key cell cycle regulatory proteins following ATR treatment. As anticipated we found that the expression of p53 and p27 proteins which were significantly upregulated in the SVZ of JEV-infected animals were noticeably reduced in JEV+ATR group. p53 is implicated in several neurodegenerative disorders including ALS, Alzheimer's and Parkinson's disease (Chang *et al.* 2012; Szybińska and Leśniak 2017). The transcriptional activity of p53 is known to be modulated by its interaction with various cellular factors which are altered during disease pathology (Chang *et al.* 2012). One such factor is a mitochondrial membrane protein known as Prohibitin (PHB) which is reported to enhance the binding of p53 to its targets thereby increasing its transcriptional activity (Fusaro *et al.* 2003). We previously found that PHB interacts with JEV RNA, although its role in JEV infection is still elusive, knockdown of PHB using siRNA has been found to affect the release of mature JEV virion from infected NSPCs (Mukherjee *et al.* 2017). ATR treatment markedly reduced PHB expression following JEV infection which, in part, might be responsible for the decline in p53 expression after ATR treatment.

Interferons are a family of cytokines dedicated to provide immunity against viruses. They induce expression of ISGs which are crucial for viral control (Crosse *et al.* 2018). IFN-β was found to be upregulated post infection and its expression was reduced following ATR treatment. However, we did not observe any significant changes in the mRNA expression of IFN-α and IFN-γ after ATR treatment. These observations corroborate with previous reports in multiple sclerosis where atorvastatin inhibited interferon-β response (Feng *et al.* 2012). Emerging evidence indicates the role of IFN-β in immunomodulation and regulation of proliferation and differentiation extending beyond its antiviral activity (Liu *et al.* 2001) (Neuhaus *et al.* 2003). Treatment of NSPCs with IFN-β is reported to limit neurosphere proliferation *in vitro* (Lum *et al.* 2009) which is in line with our observation that spheres resumed their normal sizes after ATR treatment; possibly an effect seen due to ATR facilitated decline in IFN- β.

Despite significant advances in our understanding of the JEV pathogenesis for the past decade, yet no specific treatment for JE is available till date. The protective effects of atorvastatin on NSPCs following JEV infection as reported in this study underscores its further clinical

valuation in alleviating symptoms of JE. Given the apparent contradictory role of the immune system in disease pathology, combination therapy of statins with other potential anti-inflammatory and antiviral compounds such as ribavirin, minocycline; needs strong consideration as new methods to treat Japanese encephalitis.

Acknowledgements

The study is supported by research grant to AB form Department of Biotechnology (BT/PR27796/Med/29/1301/2018). AB is also the recipient of Tata Innovation Fellowship (BT/HRD/35/01/02/2014). SM (Mallick) is also recipient of grant from Science & Engineering Research Board (SERB) (PDF/2016/000440). The authors sincerely acknowledge the help of Kanhaiya Lal Kumawat and Manish Dogra.

References

Abrous DN, Koehl M and Le Moal M 2005 Adult neurogenesis: from precursors to network and physiology. *Physiol. Rev.* **85** 523–569

Aktas O, Waiczies S, Smorodchenko A, Dorr J, Seeger B *et al.* 2003 Treatment of relapsing paralysis in experimental encephalomyelitis by targeting Th1 cells through atorvastatin. *J. Exp. Med.* **197** 725–733

Amarenco P, Bogousslavsky J, Callahan A, 3rd, Goldstein LB, Hennerici M *et al.* 2006 High-dose atorvastatin after stroke or transient ischemic attack. *N. Engl. J. Med.* **355** 549–559

Arvidsson A, Collin T, Kirik D, Kokaia Z and Lindvall O 2002 Neuronal replacement from endogenous precursors in the adult brain after stroke. *Nat. Med.* **8** 963–970

Basu A and Dutta K 2017 Recent advances in Japanese encephalitis. *F1000Res* **6** 259

Borsini A, Zunszain PA, Thuret S and Pariante CM 2015 The role of inflammatory cytokines as key modulators of neurogenesis. *Trends Neurosci.* **38** 145–157

Cacci E, Claasen JH and Kokaia Z 2005 Microglia-derived tumor necrosis factor-alpha exaggerates death of newborn hippocampal progenitor cells in vitro. *J. Neurosci. Res.* **80** 789–797

Chang JR, Ghafouri M, Mukerjee R, Bagashev A, Chabrashvili T *et al.* 2012 Role of p53 in neurodegenerative diseases. *Neurodegener. Dis.* **9** 68–80

Chataway J, Schuerer N, Alsanousi A, Chan D, MacManus D, *et al.* 2014 Effect of high-dose simvastatin on brain atrophy and disability in secondary progressive multiple sclerosis (MS-STAT): a randomised, placebo-controlled, phase 2 trial. *Lancet* **383** 2213–2221

Chen J, Zacharek A, Li A, Cui X, Roberts C *et al.* 2008 Atorvastatin promotes presenilin-1 expression and Notch1 activity and increases neural progenitor cell proliferation after stroke. *Stroke* **39** 220–226

Chen J, Zhang ZG, Li Y, Wang Y, Wang L *et al.* 2003 Statins induce angiogenesis, neurogenesis, and synaptogenesis after stroke. *Ann. Neurol.* **53** 743–751

Choi NY, Kim JY, Hwang M, Lee EH, Choi H *et al.* 2019 Atorvastatin rejuvenates neural stem cells injured by oxygen-glucose deprivation and induces neuronal differentiation through activating the PI3K/Akt and ERK pathways. *Mol. Neurobiol.* **56** 2964–2977

Crosse KM, Monson EA, Beard MR and Helbig KJ 2018 Interferon-stimulated genes as enhancers of antiviral innate immune signaling. *J. Innate. Immun.* **10** 85–93

Das S and Basu A 2008 Japanese encephalitis virus infects neural progenitor cells and decreases their proliferation. *J. Neurochem.* **106** 1624–1636

Das S, Dutta K, Kumawat KL, Ghoshal A, Adhya D *et al.* 2011 Abrogated inflammatory response promotes neurogenesis in a murine model of Japanese encephalitis. *PLoS One* **6** e17225

Dufek M, Rektorova I, Thon V, Lokaj J and Rektor I 2015 Interleukin-6 May contribute to mortality in Parkinson's disease patients: a 4-year prospective study. *Parkinsons Dis.* **2015** 898192

Ekdahl CT, Claasen JH, Bonde S, Kokaia Z and Lindvall O 2003 Inflammation is detrimental for neurogenesis in adult brain. *Proc. Natl. Acad. Sci. USA* **100** 13632–13637

Feng X, Han D, Kilaru BK, Franek BS, Niewold TB, *et al.* 2012 Inhibition of interferon-beta responses in multiple sclerosis immune cells associated with high-dose statins. *Arch. Neurol.* **69** 1303–1309

Fusaro G, Dasgupta P, Rastogi S, Joshi B and Chellappan S 2003 Prohibitin induces the transcriptional activity of p53 and is exported from the nucleus upon apoptotic signaling. *J. Biol. Chem.* **278** 47853–47861

Ghoshal A, Das S, Ghosh S, Mishra MK, Sharma V *et al.* 2007 Proinflammatory mediators released by activated microglia induces neuronal death in Japanese encephalitis. *Glia* **55** 483–496

Göritz C and Frisén J 2012 Neural stem cells and neurogenesis in the adult. *Cell. Stem. Cell.* **10** 657–659

Iosif RE, Ekdahl CT, Ahlenius H, Pronk CJ, Bonde S *et al.* 2006 Tumor necrosis factor receptor 1 is a negative regulator of progenitor proliferation in adult hippocampal neurogenesis. *J. Neurosci.* **26** 9703–9712

Ishikawa T and Konishi E 2015 Potential chemotherapeutic targets for Japanese encephalitis: current status of antiviral drug development and future challenges. *Expert. Opin. Ther. Targets.* **19** 1379–1395

Kumar R, Basu A, Sinha S, Das M, Tripathi P *et al.* 2016 Role of oral Minocycline in acute encephalitis syndrome in India - a randomized controlled trial. *BMC Infect. Dis.* **16** 67

Kumar R, Tripathi P, Baranwal M, Singh S, Tripathi S *et al.* 2009 Randomized, controlled trial of oral ribavirin for Japanese encephalitis in children in Uttar Pradesh, India. *Clin. Infect. Dis.* **48** 400–406

Lee SH, Choi NY, Yu HJ, Park J, Choi H *et al.* 2016 Atorvastatin protects NSC-34 motor neurons against oxidative stress by activating PI3K, ERK and free radical scavenging. *Mol. Neurobiol.* **53** 695–705

Liu Z, Pelfrey CM, Cotleur A, Lee JC and Rudick RA 2001 Immunomodulatory effects of interferon beta-1a in multiple sclerosis. *J. Neuroimmunol.* **112** 153–162

Lum M, Croze E, Wagner C, McLenachan S, Mitrovic B *et al.* 2009 Inhibition of neurosphere proliferation by IFNgamma but not IFNbeta is coupled to neuronal differentiation. *J. Neuroimmunol.* **206** 32–38

Ma DK, Bonaguidi MA, Ming GL and Song H 2009 Adult neural stem cells in the mammalian central nervous system. *Cell Res.* **19** 672–682

Mallick S, Chakraborty S, Hazra B, Dev S, Mukherjee S *et al.* 2019 Novel strategy for treating neurotropic viral infections using hypolipidemic drug Atorvastatin. *bioRxiv* https://doi.org/10.1101/639096639096

Marti-Fabregas J, Romaguera-Ros M, Gomez-Pinedo U, Martinez-Ramirez S, Jimenez-Xarrie E, *et al.* 2010 Proliferation in the human ipsilateral subventricular zone after ischemic stroke. *Neurology* **74** 357–365

Martino G, Butti E and Bacigaluppi M 2014 Neurogenesis or non-neurogenesis: that is the question. *J. Clin. Invest.* **124** 970–973

Mehrbod P, Omar AR, Hair-Bejo M, Haghani A and Ideris A 2014 Mechanisms of action and efficacy of statins against influenza. *Biomed. Res. Int.* **2014** 872370

Mukherjee S, Singh N, Sengupta N, Fatima M, Seth P *et al.* 2017 Japanese encephalitis virus induces human neural stem/progenitor cell death by elevating GRP78, PHB and hnRNPC through ER stress. *Cell Death. Dis.* **8** e2556

Nazmi A, Dutta K and Basu A 2011 RIG-I mediates innate immune response in mouse neurons following Japanese encephalitis virus infection. *PLoS One* **6** e21761

Nazmi A, Mukherjee S, Kundu K, Dutta K, Mahadevan A *et al.* 2014 TLR7 is a key regulator of innate immunity against Japanese encephalitis virus infection. *Neurobiol. Dis.* **69** 235–247

Neuhaus O, Archelos JJ and Hartung HP 2003 Immunomodulation in multiple sclerosis: from immunosuppression to neuroprotection. *Trends Pharmacol. Sci.* **24** 131–138

Niimi Y and Levison SW 2018 Pediatric brain repair from endogenous neural stem cells of the subventricular zone. *Pediatr. Res.* **83** 385–396

Schweitzer BK, Chapman NM and Iwen PC 2009 Overview of the Flaviviridae with an emphasis on the Japanese encephalitis group viruses. *Lab. Med.* **40** 493–499

Seyfried D, Han Y, Lu D, Chen J, Bydon A, *et al.* 2004 Improvement in neurological outcome after administration of atorvastatin following experimental intracerebral hemorrhage in rats. *J. Neurosurg.* **101** 104–107

Shih RH, Wang CY and Yang CM 2015 NF-kappaB signaling pathways in neurological inflammation: a mini review. *Front. Mol. Neurosci.* **8** 77

Song G, Ouyang G and Bao S 2005 The activation of Akt/PKB signaling pathway and cell survival. *J. Cell. Mol. Med.* **9** 59–71

Sparks DL, Connor DJ, Browne PJ, Lopez JE and Sabbagh MN 2002 HMG-CoA reductase inhibitors (statins) in the treatment of Alzheimer's disease and why it would be ill-advise to use one that crosses the blood-brain barrier. *J. Nutr. Health. Aging.* **6** 324–331

Storer MA, Gallagher D, Fatt MP, Simonetta JV, Kaplan DR, *et al.* 2018 Interleukin-6 regulates adult neural stem cell numbers during normal and abnormal post-natal development. *Stem. Cell. Rep.* **10** 1464–1480

Szybińska A and Leśniak W 2017 P53 Dysfunction in neurodegenerative diseases - the cause or effect of pathological changes? *Aging Dis.* **8** 506–518

Turtle L and Solomon T 2018 Japanese encephalitis - the prospects for new treatments. *Nat. Rev. Neurol.* **14** 298–313

Wang KW, Wang HK, Chen HJ, Liliang PC, Liang CL, *et al.* 2014 Simvastatin combined with antioxidant attenuates the cerebral vascular endothelial inflammatory response in a rat traumatic brain injury. *Biomed. Res. Int.* **2014** 910260

Wang S, Liu Y, Guo J, Wang P, Zhang L, *et al.* 2017 Screening of FDA-approved drugs for inhibitors of Japanese encephalitis virus infection. *J. Virol.* **91** e01055–17

Corresponding editor: Saumitra Das